DTU Library

Evaluating and improving WAsP using tall wind measurements

Floors, Rogier Ralph; Troen, Ib; Kelly, Mark C.; Pena Diaz, Alfredo; Gryning, Sven-Erik

Publication date:
2015

Document Version
Peer reviewed version

Evaluating and improving WAsP using tall wind measurements

Rogier Floors Ib Troen Mark Kelly Alfredo Peña Sven-Erik Gryning

DTU Wind Energy, Risø campus – Department of Wind Energy

EMS 2015, Sofia, Bulgaria, Energy Meteorology session

The WAsP (Wind Atlas Software Program) profile model

- Based on the Weibull distribution, with parameters A (scale) and k (shape).

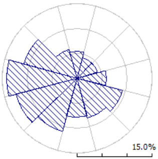

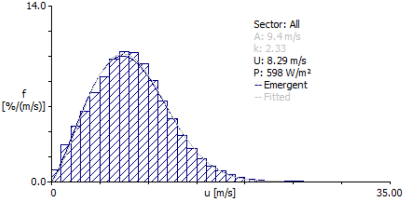

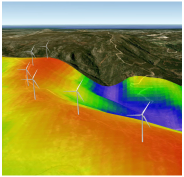

[1]See poster P26 "Full-scale wind lidar measurements of the shelter behind a fence"

The WAsP (Wind Atlas Software Program) profile model

- Based on the Weibull distribution, with parameters A (scale) and k (shape).
- Contains orographic model, roughness change model, shelter model[1], wake model and vertical profile model.

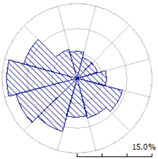

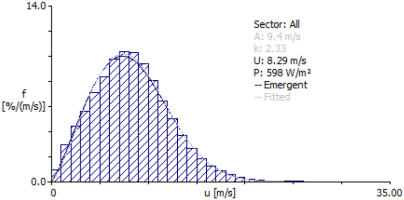

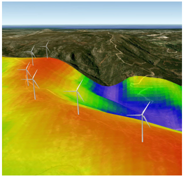

[1] See poster P26 "Full-scale wind lidar measurements of the shelter behind a fence"

The WAsP (Wind Atlas Software Program) profile model

- Based on the Weibull distribution, with parameters A (scale) and k (shape).
- Contains orographic model, roughness change model, shelter model[1], wake model and vertical profile model.
- Extensively used worldwide for wind resource estimations (4500 users, 6000+ turbines sited)

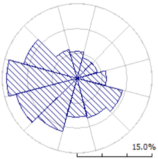

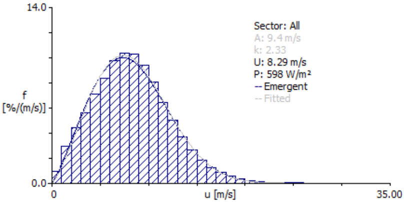

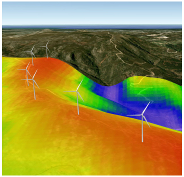

[1] See poster P26 "Full-scale wind lidar measurements of the shelter behind a fence"

Introduction

Motivation: 'tall' turbines reach above the surface layer and large-scale processes become more important at these heights.

- **Improve the profile model in WAsP for both wind speed ($U = A\Gamma(1 + 1/k)$) and power density ($E = \frac{1}{2}\rho A^3\Gamma\left(1 + 3/k\right)$)**

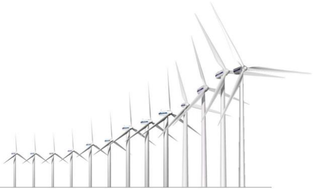

Product/Rotor diameter (m)	V15	V17	V19	V20	V25	V27	V39	V44	V47	V52	V66	V80	V90
Year of installation	1981	1984	1986	1987	1988	1989	1991	1995	1997	2000	1999	2000	2002
Capacity (kW)	55	75	90	100	200	225	500	600	660	850	1750	2000	3000
MWh/year	217	265	301	346	481	647	1304	1581	1947	2530	4705	6768	9152

Introduction

Motivation: 'tall' turbines reach above the surface layer and large-scale processes become more important at these heights.

- **Improve the profile model in WAsP for both wind speed ($U = A\Gamma(1+1/k)$) and power density ($E = \frac{1}{2}\rho A^3 \Gamma\left(1+3/k\right)$)**
- Major research efforts to improve vertical profile model

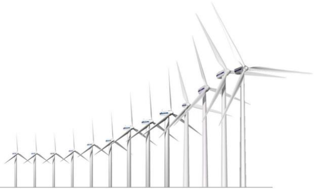

Product/Rotor diameter (m)	V15	V17	V19	V20	V25	V27	V39	V44	V47	V52	V66	V80	V90
Year of installation	1981	1984	1986	1987	1988	1989	1991	1995	1997	2000	1999	2000	2002
Capacity (kW)	55	75	90	100	200	225	500	600	660	850	1750	2000	3000
MWh/year	217	265	301	346	481	647	1304	1581	1947	2530	4705	6768	9152

Introduction

Motivation: 'tall' turbines reach above the surface layer and large-scale processes become more important at these heights.

- **Improve the profile model in WAsP for both wind speed ($U = A\Gamma(1 + 1/k)$) and power density ($E = \frac{1}{2}\rho A^3\Gamma\left(1 + 3/k\right)$)**
- Major research efforts to improve vertical profile model
- Use measurements from 3 tall wind sites for parameter estimation

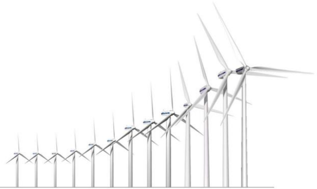

Product/Rotor diameter (m)	V15	V17	V19	V20	V25	V27	V39	V44	V47	V52	V66	V80	V90
Year of installation	1981	1984	1986	1987	1988	1989	1991	1995	1997	2000	1999	2000	2002
Capacity (kW)	55	75	90	100	200	225	500	600	660	850	1750	2000	3000
MWh/year	217	265	301	346	481	647	1304	1581	1947	2530	4705	6768	9152

Introduction

Motivation: 'tall' turbines reach above the surface layer and large-scale processes become more important at these heights.

- **Improve the profile model in WAsP for both wind speed ($U = A\Gamma(1 + 1/k)$) and power density ($E = \frac{1}{2}\rho A^3\Gamma(1 + 3/k)$)**
- Major research efforts to improve vertical profile model
- Use measurements from 3 tall wind sites for parameter estimation
- Implementation of baroclinicity effects from CFSR data

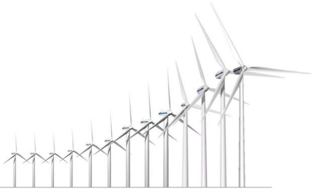

Product/Rotor diameter (m)	V15	V17	V19	V20	V25	V27	V39	V44	V47	V52	V66	V80	V90
Year of installation	1981	1984	1986	1987	1988	1989	1991	1995	1997	2000	1999	2000	2002
Capacity (kW)	55	75	90	100	200	225	500	600	660	850	1750	2000	3000
MWh/year	217	265	301	346	481	647	1304	1581	1947	2530	4705	6768	9152

Introduction

Motivation: 'tall' turbines reach above the surface layer and large-scale processes become more important at these heights.

- **Improve the profile model in WAsP for both wind speed ($U = A\Gamma(1 + 1/k)$) and power density ($E = \frac{1}{2}\rho A^3 \Gamma\left(1 + 3/k\right)$)**
- Major research efforts to improve vertical profile model
- Use measurements from 3 tall wind sites for parameter estimation
- Implementation of baroclinicity effects from CFSR data
- Evaluation using 28 meteorological masts

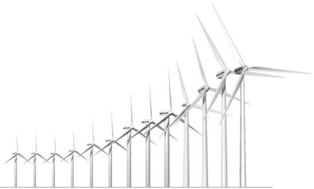

Product/Rotor diameter (m)	V15	V17	V19	V20	V25	V27	V39	V44	V47	V52	V66	V80	V90
Year of installation	1981	1984	1986	1987	1988	1989	1991	1995	1997	2000	1999	2000	2002
Capacity (kW)	55	75	90	100	200	225	500	600	660	850	1750	2000	3000
MWh/year	217	265	301	346	481	647	1304	1581	1947	2530	4705	6768	9152

Main ingredients from wind profile model in WAsP

WAsP models the effect of stability by using the logarithmic wind profile and the geostrophic drag law,

$$\frac{U}{u_*} = \frac{1}{\kappa}\left[\ln\left(\frac{z}{z_0}\right) - \psi_m\left(\frac{z}{L}\right)\right] \tag{1}$$

$$\frac{G}{u_*} = \frac{1}{\kappa}\sqrt{\left[\ln\left(\frac{u_*}{fz_0}\right) + A\right]^2 + B^2} \tag{2}$$

A and B are functions of internal stability parameter $(\mu \equiv \kappa u_*/fL)$
A first-order expansion in heatflux H is used for a u_* offset from neutral,

$$\frac{du_*}{u_*} = \frac{cg}{fT_0 c_p \rho G^2} dH \tag{3}$$

with

$$c = B\frac{dB}{d\mu} - \left(\ln \mathrm{Ro} + \ln\frac{u_*}{G} - A\right)\frac{dA}{d\mu}, \tag{4}$$

In WAsP c is assumed constant and ≈ 2.5. c also influences the reversal height, the height where there is maximum in the k parameter of the Weibull distribution. Consistent way of treating H_{off} and H_{rms}.

Wind lidar measurements

- $G =$ wind lidar wind speed 950 m ($h \ll 950$ m)

Measurements described in Floors, R., Peña, A., and Gryning, S.-E. (2015a). The effect of baroclinicity on the wind in the planetary boundary layer.
Quarterly Journal of the Royal Meteorological Society, 141(687):619–630

Wind lidar measurements

- G = wind lidar wind speed 950 m ($h \ll 950$ m)
- α = veering angle from mast + veering angle from lidar

Measurements described in Floors, R., Peña, A., and Gryning, S.-E. (2015a). The effect of baroclinicity on the wind in the planetary boundary layer.
Quarterly Journal of the Royal Meteorological Society, 141(687):619–630

Wind lidar measurements

- G = wind lidar wind speed 950 m ($h \ll 950$ m)
- α = veering angle from mast + veering angle from lidar
- z_0 = 0.03 m Høvsøre, 0.5 m Hamburg, 0.0002 m Fino

Measurements described in Floors, R., Peña, A., and Gryning, S.-E. (2015a). The effect of baroclinicity on the wind in the planetary boundary layer.
Quarterly Journal of the Royal Meteorological Society, 141(687):619–630

Wind lidar measurements

- G = wind lidar wind speed 950 m ($h \ll 950$ m)
- α = veering angle from mast + veering angle from lidar
- z_0 = 0.03 m Høvsøre, 0.5 m Hamburg, 0.0002 m Fino
- u_* = iteratively solving diabatic wind profile for u_*, θ_*, q_*, L based on temperature, humidity and wind profile

Measurements described in Floors, R., Peña, A., and Gryning, S.-E. (2015a). The effect of baroclinicity on the wind in the planetary boundary layer.
Quarterly Journal of the Royal Meteorological Society, 141(687):619–630

Stability $dA/d\mu$ and $dB/d\mu$ in near-neutral conditions

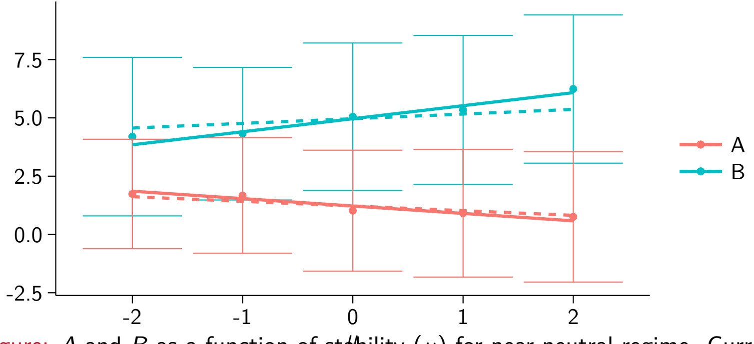

Figure: A and B as a function of stability (μ) for near neutral regime. Current linearizations used in WAsP (± 0.2) shown with dashed lines

Neutral A and B and wind direction

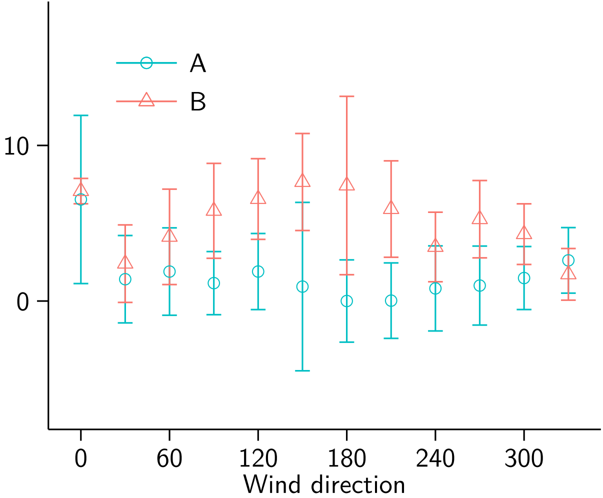

Figure: Neutral observations A and B, error bars denoting the standard deviation in each 30° bin. **Why dependent on wind direction?**

Baroclinic wind profile in theory

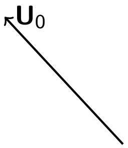

a)

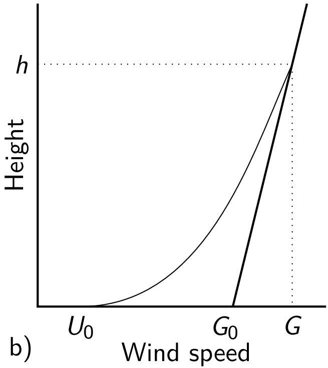

b)

Baroclinic wind profile in theory

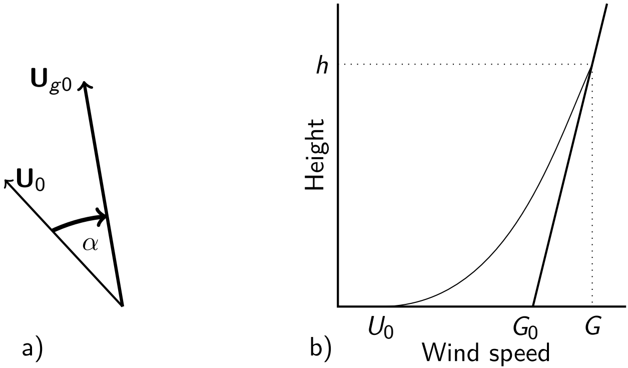

$\theta = \arctan(V_g/U_g)$ = geostrophic wind direction

Baroclinic wind profile in theory

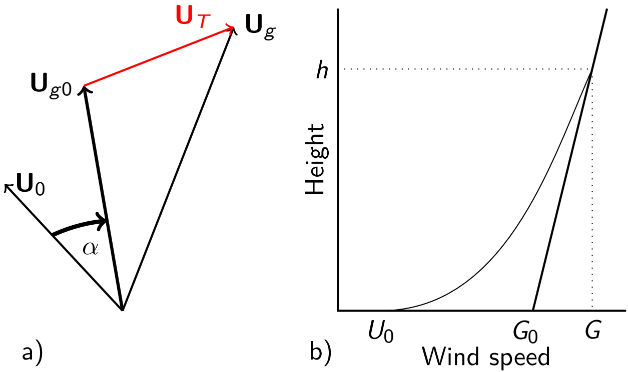

$$\theta = \arctan(V_g/U_g) = \text{geostrophic wind direction}$$

$$\gamma = \arctan\left(\frac{dV_g}{dz}/\frac{dU_g}{dz}\right) = \text{long-term mean thermal wind direction}$$

Baroclinic wind profile in theory

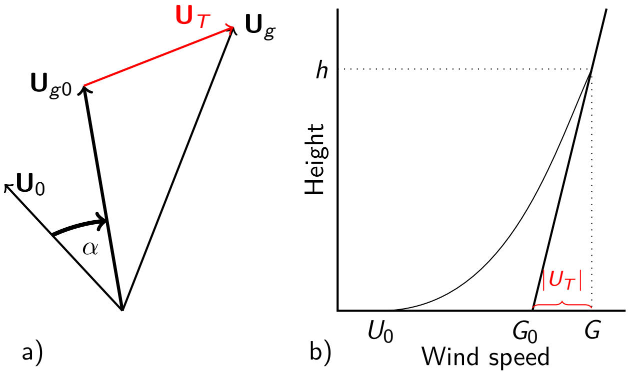

$$\theta = \arctan(V_g/U_g) = \text{geostrophic wind direction}$$

$$\gamma = \arctan\left(\frac{dV_g}{dz} / \frac{dU_g}{dz}\right) = \text{long-term mean thermal wind direction}$$

$$M_0 = \frac{\kappa^2}{f} \frac{d|U_T|}{dz} = \text{long-term dimensionless geostrophic shear}$$

Modelling the effect of baroclinicity

A and B also function of baroclinicity,

$$A = A_0 + A' = A_0 + M_0 \cos(\theta - \gamma - \alpha), \tag{5}$$

$$B = B_0 + B' = B_0 + M_0 \sin(\theta - \gamma - \alpha), \tag{6}$$

- Eq. 5 and 6 were implemented in WAsP
- Thermal wind vector is obtained from CFSR data from geopotential height fields at 1000 and 950 hPa ($\pm$ 0–500 m)

θ = surface wind direction
γ = long-term mean thermal wind direction
M_0 = long-term dimensionless geostrophic shear
α = wind veer in boundary-layer

Baroclinicity and A and B

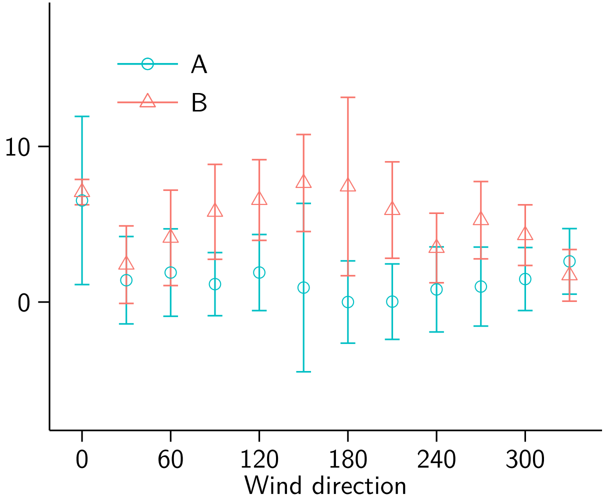

Figure: Observations A and B, error bars denoting the standard deviation in each 30° bin. The lines denote Eqs. 5 and 6 using $M_0 = 2.2$ and $\gamma = 300°$, obtained from CFSR data.

Baroclinicity and *A* and *B*

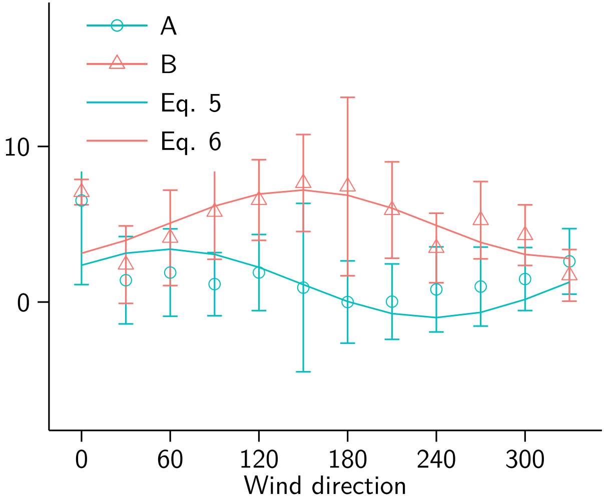

Figure: Observations A and B, error bars denoting the standard deviation in each 30° bin. The lines denote Eqs. 5 and 6 using $M_0 = 2.2$ and $\gamma = 300°$, obtained from CFSR data.

Evaluating the models

1. WAsP 11.4 (Troen and Petersen, 1989)

Evaluating the models

1. WAsP 11.4 (Troen and Petersen, 1989)
2. 'Kelly et al.' profile model (Gryning et al., 2007; Kelly and Gryning, 2010; Kelly et al., 2014)

Evaluating the models

1. WAsP 11.4 (Troen and Petersen, 1989)
2. 'Kelly et al.' profile model (Gryning et al., 2007; Kelly and Gryning, 2010; Kelly et al., 2014)
3. Exact solutions + baroclincity from CFSR (Troen and Petersen, 1989; Floors et al., 2015b)

Error metrics

- Mean absolute relative error, root-mean-square relative error

Error metrics

- Mean absolute relative error, root-mean-square relative error
- Both for wind speed U and power density E

Error metrics

- Mean absolute relative error, root-mean-square relative error
- Both for wind speed U and power density E
- Cross predictions upwards (i.e. 10-40, 40-100 and 10-100 m)

Error metrics

- Mean absolute relative error, root-mean-square relative error
- Both for wind speed U and power density E
- Cross predictions upwards (i.e. 10-40, 40-100 and 10-100 m)
- Exclude tall wind measurements, total of 28 sites

Sites

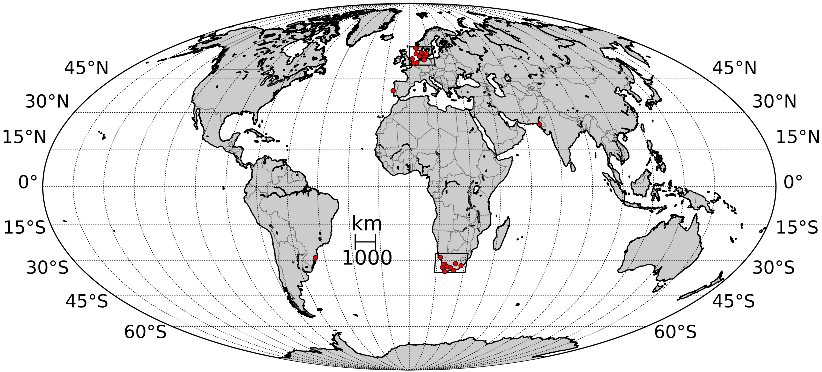

Figure: Overview of sites used for the model evaluation.

Sites

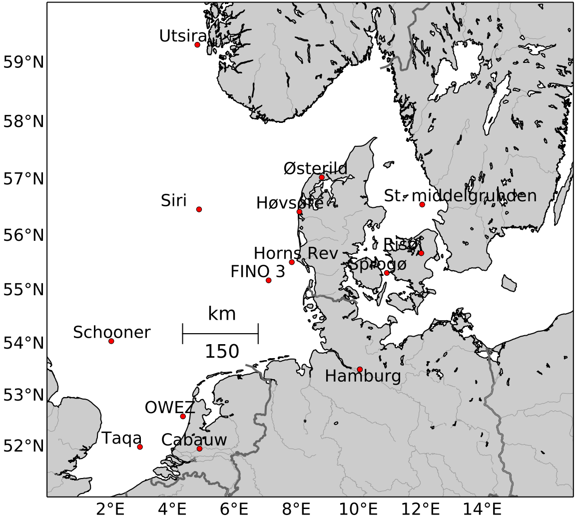

Figure: Overview of sites near Denmark.

Sites

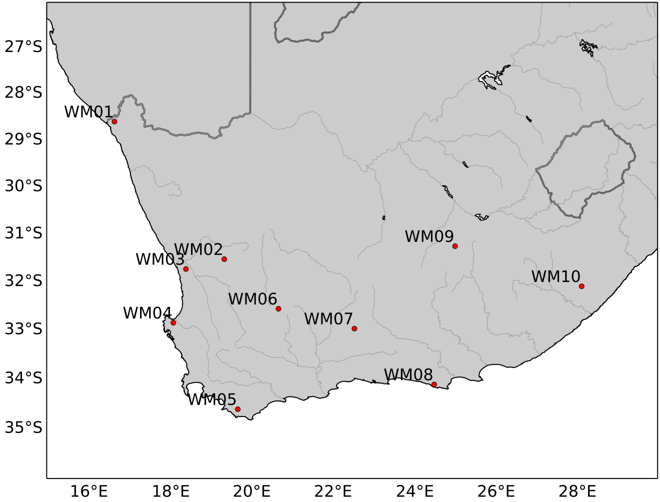

Figure: Overview of sites in South Africa.

Optimization using new default stability settings

Because the stability treatment in the model is now different, we optimized models to find values of H_{off} and H_{rms} that minimized RMSE in U and E

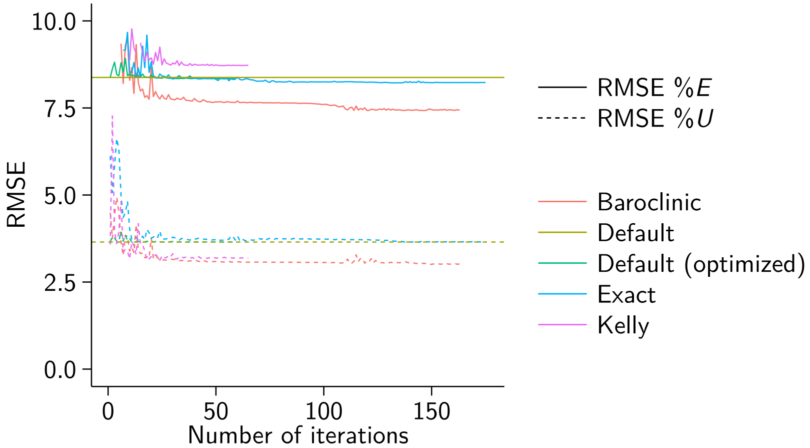

Conclusions

1. Climatological impact of baroclinicity has distinct impact on geostrophic drag law

Conclusions

1. Climatological impact of baroclinicity has distinct impact on geostrophic drag law
2. Implemented baroclinicity using just two additional parameters for each site from CFSR data

Conclusions

1. Climatological impact of baroclinicity has distinct impact on geostrophic drag law
2. Implemented baroclinicity using just two additional parameters for each site from CFSR data
3. Baroclinicty + exact model approximately 10-20 % better than old model in all error metrics

Conclusions

1. Climatological impact of baroclinicity has distinct impact on geostrophic drag law
2. Implemented baroclinicity using just two additional parameters for each site from CFSR data
3. Baroclinicty + exact model approximately 10-20 % better than old model in all error metrics
4. Improvements most easily visible at 'tall' extrapolations

Thank you for your attention.

The study is supported by the Danish Research Agency Strategic Research Council (Sagsnr. 2104-08-0025) “Tall wind” project and internal funding. We acknowledge the BMU sponsered FINO3 mast project for the mast measurements and the Test & Measurement department for processing all measurements. We also acknowledge NCEP for the CFSR data set.

Floors, R., Peña, A., and Gryning, S.-E. (2015a). The effect of baroclinicity on the wind in the planetary boundary layer. *Quarterly Journal of the Royal Meteorological Society*, 141(687):619–630.

Floors, R., Troen, I., and Kelly, M. C. (2015b). Evaluating and improving WAsP using 'tall' wind measurements. *Wind Energy*, in prep.

Gryning, S.-E., Batchvarova, E., Brümmer, B., Jørgensen, H., and Larsen, S. (2007). On the extension of the wind profile over homogeneous terrain beyond the surface boundary layer. *Boundary-Layer Meteorol.*, 124(2):251–268.

Kelly, M. and Gryning, S.-E. (2010). Long-Term Mean Wind Profiles Based on Similarity Theory. *Boundary-Layer Meteorology*, 136(3):377–390.

Kelly, M., Troen, I., and Jørgensen, H. E. (2014). Weibull-k Revisited: "Tall" Profiles and Height Variation of Wind Statistics. *Boundary-Layer Meteorology*, 152(1):107–124.

Troen, I. and Petersen, E. L. (1989). *European Wind Atlas*. Risø National Laboratory, Roskilde, Denmark.

Saha, Suranjana, and Coauthors (2014). The NCEP Climate Forecast System Version 2. J.

Climate, 27, 2185-2208